DATE ISSUED OCT 11 1978

ORNL-5431

780517

Effect of Oxidizing Environment on Mechanical Properties of Molybdenum and TZM

C. T. Liu
S. H. Anderson
H. Inouye

OAK RIDGE NATIONAL LABORATORY
OPERATED BY UNION CARBIDE CORPORATION · FOR THE DEPARTMENT OF ENERGY

Printed in the United States of America. Available from
National Technical Information Service
U.S. Department of Commerce
5285 Port Royal Road, Springfield, Virginia 22161
Price: Printed Copy $4.50; Microfiche $3.00

ORNL-5431
Distribution
Category UC-25

Contract No. W-7405-eng-26

METALS AND CERAMICS DIVISION

EFFECT OF OXIDIZING ENVIRONMENT ON MECHANICAL PROPERTIES OF MOLYBDENUM AND TZM

C. T. Liu, S. H. Anderson, and H. Inouye

Date Published: October 1978

OAK RIDGE NATIONAL LABORATORY
Oak Ridge, Tennessee 37830
operated by
UNION CARBIDE CORPORATION
for the
DEPARTMENT OF ENERGY

CONTENTS

EFFECT OF OXIDIZING ENVIRONMENT ON MECHANICAL PROPERTIES OF MOLYBDENUM AND TZM

C. T. Liu, S. H. Anderson,[1] and H. Inouye

ABSTRACT

The effect of environment on mechanical properties of molybdenum and TZM was investigated in low-pressure (1.3-mPa) oxygen at 1150°C. Specimens of TZM picked up oxygen and lost carbon. The oxygen concentration increases linearly with exposure time, indicating that the chemisorption of oxygen molecules at the specimen surface, rather than bulk diffusion, controls the kinetics of oxygen absorption at 1150°C. Specimens of TZM increase in tensile strength and decrease in ductility with increasing oxygen content. Exposed TZM loses its ductility at elevated temperatures at an oxygen level of 500 ppm. The embrittlement is due to the formation of zones or oxide precipitates, which harden the alloy and promote the brittle fracture associated with cleavage and grain-boundary separation.

Unalloyed molybdenum responds to the oxidizing environment quite differently from TZM. The molybdenum (containing no active element such as Ti and Zr) showed no internal oxidation at 1150°C. Instead, our results indicate that a trace of oxygen penetrated into molybdenum through its grain boundaries. This penetration raises the ductile-to-brittle transition temperature of molybdenum by 200°C and lowers the ductility above 900°C. The ductility of oxygen-exposed molybdenum is virtually unaffected in the temperature range from 400 to 900°C. A ductility minimum (10%) is observed at 1350°C because of dynamic embrittlement effects; that is, diffusion of oxygen to grain boundaries or crack tips where high triaxial states of stress are generated during plastic deformation. This embrittlement can be totally eliminated by an increase in strain rate.

INTRODUCTION

Structural materials for closed-cycle energy-conversion systems, such as gas-cooled reactor and space power systems, are required to maintain adequate strength and ductility during service in slightly contaminated environments at elevated temperatures. The environments of such power

---

[1] Summer employee 1975 and 1977. Present address, Carnegie-Mellon University, Pittsburgh, Pa.

systems operating at temperatures above 700°C generally consist of helium and/or argon plus low-pressure active gases derived from decomposition of oxide fuels and outgassing of graphite and insulation materials.

Molybdenum-base alloys, such as TZM (Mo—0.5% Ti—0.05% Zr—0.02% C), are considered as potential structural alloys for these applications. This is because they have adequate high-temperature strength and are relatively unreactive in terms of the permeability and solubility of interstitial impurities such as C, N, and O. A previous study found[2] that TZM picked up oxygen on exposure to O_2, CO, and H_2O at 825 and 1000°C. The rate of oxygen absorption depended strongly on the reaction temperature and was insensitive to the gas pressure and species at 825°C. The alloy showed a moderate reduction in ductility after exposure for 2000 h at 850°C but lost its ductility completely after a short exposure at 1000°C.

The current work on TZM and molybdenum is an extension of our prior studies. We previously found[2] that a diffusion process controls the kinetics of the oxygen absorption at 825°C, while bulk diffusion and gas-metal interaction at the specimen surface both affect the rate at 1000°C. The chemisorption process tends to become more prominent as the rate-controlling step with increasing reaction temperature.

The first objective of this study is to characterize the oxygen-absorption behavior of TZM at a higher temperature, such as 1150°C. The oxygen absorbed in TZM reacts with titanium and zirconium to form oxide particles whose size and coherency depend on the reaction temperature. The embrittlement in exposed TZM is mainly due to the hardening of grains through precipitation of oxide particles. The hardening effect will be reduced if the reaction temperature is high enough to coarsen the oxide particles during exposure. Thus, the second objective of this study is to determine whether TZM can tolerate more oxygen when oxidized at 1150°C. The third objective of this study is to characterize the environmental effects on the mechanical properties of molybdenum to better understand the role of alloying elements in

---

[2] C. T. Liu and H. Inouye, "Internal Oxidation and Mechanical Properties of TZM-Mo Alloy," *Metall. Trans.* 5: 2515—25 (1974).

oxidation response. The ultimate goal of our study is to identify the molybdenum-base alloys that are insensitive to the contaminated environments in the closed-cycle energy systems.

In this study, 0.51-mm-thick sheet specimens of molybdenum and TZM were exposed to low-pressure oxygen at 1150°C. The tensile properties of both control and exposed specimens were determined at temperatures to 1450°C, and their fracture behavior was examined by optical and scanning electron microscopy. The results are discussed in terms of absorption and distribution of oxygen and precipitation of oxides in TZM and molybdenum.

EXPERIMENTAL PROCEDURES

Coupon specimens (25 by 13 mm) and tensile specimens (with a gage section 12.7 by 3.2 mm) were blanked from 0.53-mm-thick molybdenum and TZM sheets obtained from Climax Molybdenum Company. To remove milling scale and surface oxide, the specimens were first chemically polished in a solution of 30 ml lactic acid, 10 ml HNO_3, and 5 ml HF, then electropolished in a solution of 800 ml methanol, 180 ml H_2SO_4, and 20 ml HF at 7—8 V for about 30 s. For some specimens mechanical polishing with 320-grit SiC paper was used before chemical etching to get a flatter surface and better finish. The specimens were then given a 1-h recrystallization anneal, molybdenum at 1200°C and TZM at 1600°C, in a vacuum furnace at pressures less than 0.1 mPa. The tensile specimens were re-electropolished for 90 s to remove surface scratches and obtain good and consistent ductility at room temperature. Table 1 shows the chemical composition of TZM and molybdenum after recrystallization.

The specimens were exposed to an oxygen pressure of 1.3 mPa (1×10^{-5} torr) at 1150°C in a 57-mm-diam mullite tube furnace. The base pressure in the vacuum system was about 25 μPa, and the oxygen pressure was maintained by a constant leak monitored by a hot-filament ion gage. The temperature was monitored by a Pt vs Pt—10% Rh thermocouple located in the center of the furance. The vacuum was maintained by an oil diffucion pump with a liquid-nitrogen trap between the hot zone and the diffusion pump. As a control test, molybdenum specimens were also aged at 1150°C in a high vacuum (0.1 μPa).

Table 1. Chemical Composition of TZM and Molybdenum Used in Study

Element	Content[a]			
	TZM			Mo
	(wt %)	(at. %)	(wt ppm)	(wt ppm)
Ti	0.51	1.01		
Zr	0.054	0.057		
C			177	48
O			20	21
N			5	4
H			3	7
Fe				<30
Ni				<10
Si				<20

[a] Balance, Mo.

The extent of oxidation was controlled by exposure time, which varied from 5 to 1000 h. After exposure, the specimens were removed for mechanical testing and chemical analysis (by Leco carbon and vacuum fusion methods). Purplish-brown oxide coatings that formed on the coupon surface were removed by a brief electropolishing before chemical analysis.

Mechanical testing was done on an Instron testing machine at a crosshead speed of 2.5 mm/min. To perform the tensile test at elevated temperatures, a water-cooled quartz-tube vacuum system was attached to the Instron testing machine, and specimens were heated by radiation from an inductively heated tantalum susceptor under a vacuum of about 0.1 mPa. Temperatures were determined with a Pt vs Pt—10% Rh thermocouple located at the center of the specimen. The load-time curves were recorded automatically and were used to generate the stress-strain data. Fracture sufraces were examined with a JSM-U3 scanning electron microscope operated at 25 kV. Fracture surface areas were measured with a Nikon Measurscope equipped with a EPI Electromike digital readout.

RESULTS

Change in Interstitial Composition

Table 2 lists the interstitial contents in molybdenum and TZM determined by chemical analysis. Coupons of TZM show a steady increase in oxygen content and decrease in carbon content with reaction time. The carbon content decreases from 177 to 43 ppm after 100-h exposure at 1150°C, while the nitrogen and hydrogen contents do not change with exposure. Figure 1 shows the oxygen and carbon contents in TZM as functions of exposure time. The oxygen content increases linearly with time at a rate of about 20 ppm/h. The interstitial contents in unalloyed molybdenum do not change significantly with exposure to 1.3 mPa O_2 at 1150°C, as indicated in Table 2.

Table 2. Interstitial Concentrations of TZM and Molybdenum Specimens[a] Exposed to 1.3 mPa O_2 at 1150°C

Material	Exposure (h)	Interstitial Content (wt ppm)			
		O	C	N	H
TZM	0[b]	20	177	5	3
	5	115	151	6	4
	9	161	157	6	1
	16	324	143	2	4
	24	489	101	3	1
	100	2080	43	6	12
Mo	0[b]	21	48	4	7
	100	37	35	5	3
	212		49	1	3
	512	21	35	1	4
	612	21	39	1	3

[a] A purplish-brown film formed on the specimens exposed to oxygen at 1150°C and was removed by electropolishing before chemical analysis.

[b] As-recrystallized condition.

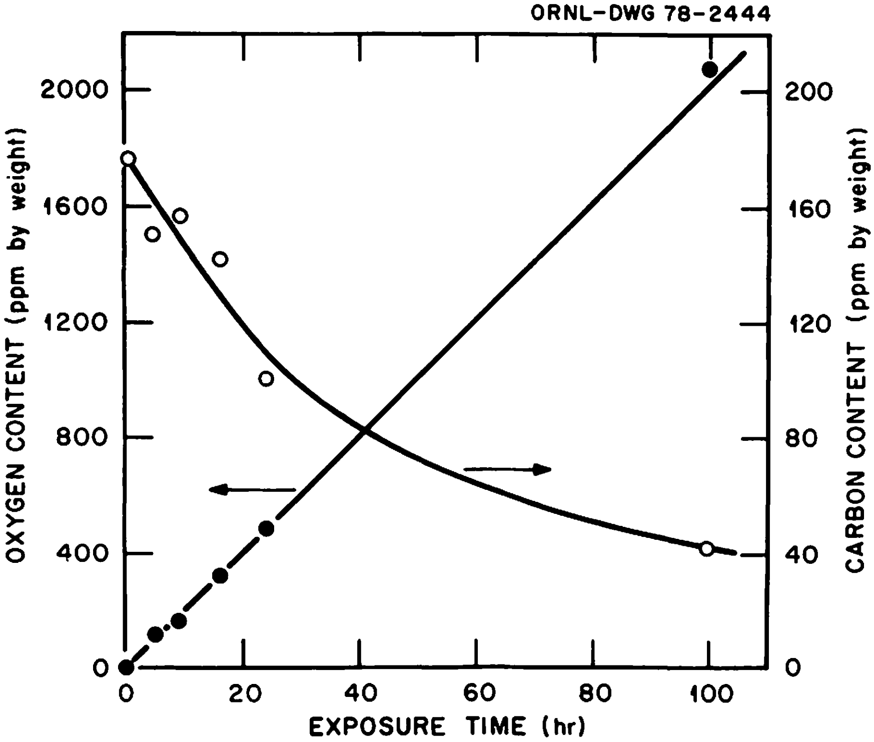

Fig. 1. Oxygen and Carbon Concentrations in TZM as Functions of Exposure Time at 1150°C and 1.3 mPa O_2.

Microstructure

Recrystallization treatment at 1200°C produced an equiaxed grain structure in the molybdenum specimens. Grain growth was evident in molybdenum after exposure to oxygen at 1150°C. The recrystallized grain size was about ASTM 7, while the grain size in the 1000-h-exposed specimens was about ASTM 6. In the molybdenum specimens exposed longer than 200 h, a few inclusions, most probably oxide, were visible along grain boundaries (Fig. 2). Even after 1000-h exposure, however, such inclusions were not seen more than one grain layer below the surface. Recrystallization at 1600°C produced an elongated fine-grain structure in TZM. Some particles, probably carbides, were seen in the as-recrystallized TZM specimens. However, the particles disappeared near the surface of the exposed specimens (Fig. 3), probably by decarburization, as indicated in Table 2.

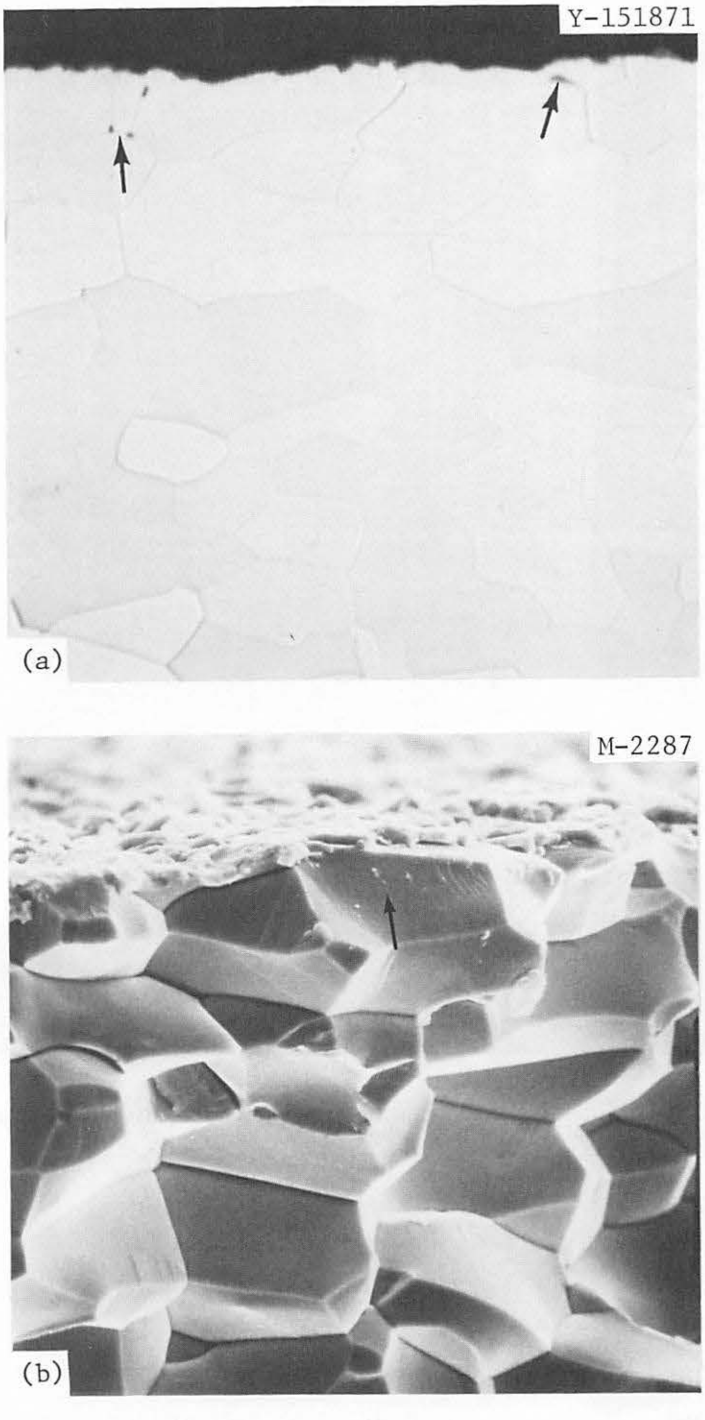

Fig. 2. Oxide Inclusions Located on Grain Boundaries Below the Surface of the Molybdenum Specimen Exposed to Oxygen for 612 h at 1150°C. (a) Optical Photograph. 1000×. (b) Scanning electron micrograph. 1000×. The inclusions are noted by arrows.

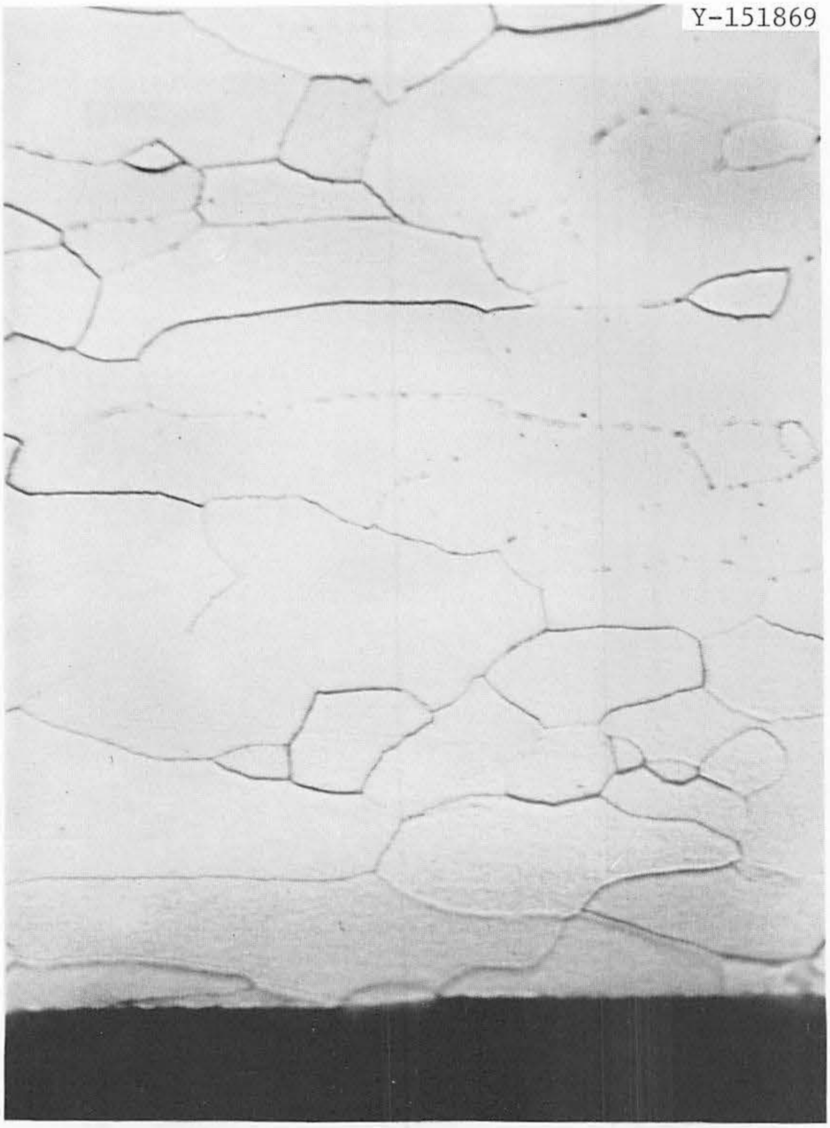

Fig. 3. Optical Microstructure of TZM Specimen Exposed to Oxygen for 100 h at 1150°C. 750×.

Tensile Properties

Molybdenum and TZM specimens either exposed to oxygen at a pressure of 1.3 mPa or aged in a high vacuum of 0.1 μPa (control specimens) at 1150°C were tensile tested in air at room temperature and in vacuum at 850, 1000, and 1150°C. A few tests were run as high as 1450°C to verify the ductility drop, which appeared in oxygen-exposed molybdenum. All the tensile data are presented in terms of exposure time and test temperature in Tables 3 through 7.

Table 3. Tensile Properties of 0.51-mm TZM Sheet Specimens Exposed to Oxygen at 1150°C and 1.3 mPa (1 × 10^{-5} torr).

Test Temperature (°C)	Exposure (h)	Elongation (%)	Strength, MPa	
			Yield	Tensile
Room	0	47	447.9	578.8
	0	41	420.3	558.1
	5	[a]		
	9	[a]		330.7
	100	[a]		
850	0	29	137.8	289.4
	5	20	220.5	330.7
	9	9	220.5	310.1
	16	7	337.6	372.1
	24	[a]	372.1	372.1
	100	[a]	379.0	379.0
1000	0	38	124.0	282.5
	5	14	199.8	296.3
	5	11	213.6	296.3
	9	10	227.4	282.5
	16	7	289.4	316.9
	24	5	275.6	296.3
	100	[a]		323.8
1150	0	37	124.0	275.6
	5	13	186.0	241.1
	9	12	179.1	241.2
	16	5	227.4	227.4
	24	6	268.7	268.7
	100	[a]		206.7

[a] Fracture before macroscopic yielding.

Table 4. Tensile Properties of 0.51-mm-Thick Molybdenum Sheet Specimens Exposed to Oxygen at 1150°C and 1.3 mPa (1×10^{-5} torr)

Test Temperature (°C)	Exposure (h)	Elongation (%)	Strength, MPa	
			Yield	Tensile
Room	0	47	482.3	537.4
	0	44	503.0	544.3
	100	6	468.5	530.5
	100	5	482.3	496.1
	112	0.5	475.4	475.4
	194	9	454.7	530.5
	612	[a]	358.3	358.3
850	0	56	75.8	220.5
	0	53	96.5	220.5
	100	48	55.1	206.7
	212	54	55.1	199.8
	512	49	62.0	192.9
	600	53	62.0	186.0
	612	58	55.1	199.8
1000	0	54	62.0	179.1
	100	46	75.8	165.4
	112	39	62.0	158.5
	212	41	55.1	158.5
	512	40	117.1	165.4
	512	46	96.5	158.5
	600	44	68.9	158.5
1150	0	54	55.1	124.0
	100	26	75.8	117.1
	112	27	62.0	130.9
	194	24	55.1	117.1
	194	30	48.2	110.2
	212	19	48.2	117.1
	212	22	55.1	124.0
	512	27	55.1	117.1
	600	24	48.2	110.2
	612	24	68.9	110.2
	1019	25	55.1	124.0

[a] Fracture before macroscopic yielding.

Table 5. Tensile Properties of 0.51-mm-Thick Molybdenum Sheet Aged at 1150°C in a Vacuum of 0.4 μPa

Test Temperature (°C)	Exposure (h)	Elongation (%)	Strength, MPa	
			Yield	Tensile
Room	0	47	482.3	537.4
	0	44	503.0	544.3
	100	35	454.7	537.4
	200	29	392.7	482.3
	608	10	365.2	496.1
850	0	56	75.8	220.5
	0	53	96.5	220.5
	100	51	55.1	199.8
	200	40	110.2	248.0
	598	50	96.5	248.0
1000	0	54	62.0	179.1
	100	54	82.7	165.4
	598	40	68.9	124.0
1150	0	54	55.1	124.0
	100	61	41.3	130.9
	185	55	41.3	137.8
	608	44	75.8	130.9
	1216	63	41.3	137.8

Table 6. Tensile Properties of 0.51-mm-Thick Molybdenum Sheet Exposed to 1.3 mPa (1 × 10^{-5} torr) Oxygen at 1150°C for 112 h

Test Temperature (°C)	Elongation (%)	Reduction of Area (%)	Strength, MPa	
			Yield	Tensile
20	[a]	4	475.4	475.4
100	9	4	385.8	427.2
200	29	28	220.5	406.5
300	40	68	96.5	344.5
400	46	82	89.6	303.2
500	45	94	82.7	268.7
600	44	88	96.5	248.0
700	46	93	62.0	220.5
800	44	92	68.9	199.8
900	44	93	75.8	186.0
1000	39	66	62.0	158.5
1150	27	43	62.0	130.9
1250	17	30	55.1	96.5
1350	10	11	48.2	82.7
1450	13	15	34.5	68.9

[a] Fracture before macroscopic yielding.

Table 7. Tensile Properties of 0.51-mm-Thick Molybdenum Aged 100 h at 1150°C in a Vacuum of 0.4 μPa

Test Temperature (°C)	Elongation (%)	Reduction of Area (%)	Strength, MPa	
			Yield	Tensile
20	35	37	454.7	537.4
110	45	58	434.1	489.2
300	58	85	186.0	323.8
500	49	94	130.9	268.7
700	60	96	96.5	206.7
850	51	97	55.1	199.8
1000	54	100	82.7	165.4
1150	61	99	41.3	130.9
1350	58	100	27.6	89.6

Tensile Properties of TZM

The tensile data for TZM are plotted as functions of exposure time and oxygen concentration in Fig. 4. Some room-temperature strength data are not included in the plots because the specimens were so brittle that they fractured before macroscopic yielding. The alloy shows a significant increase in yield strength, more than double at 850°C, but a slight increase in tensile strength at 850 and 1000°C. The ductility decreases rapidly with increasing exposure time at 1150°C, and TZM lost its room-temperature ductility completely within a 5-h exposure. As shown in Fig. 4, oxygen-exposed TZM retains some ductility at elevated temperatures, even after a 24-h exposure (oxygen content ≈480 ppm).

Tensile Properties of Molybdenum

Tensile data for molybdenum specimens exposed to oxygen at 1150°C are plotted as functions of exposure time in Fig. 5. The mechanical properties of molybdenum are quite different from those of TZM when compared at the same oxygen exposure. The strength and ductility of molybdenum at room temperature both decrease with exposure time, and

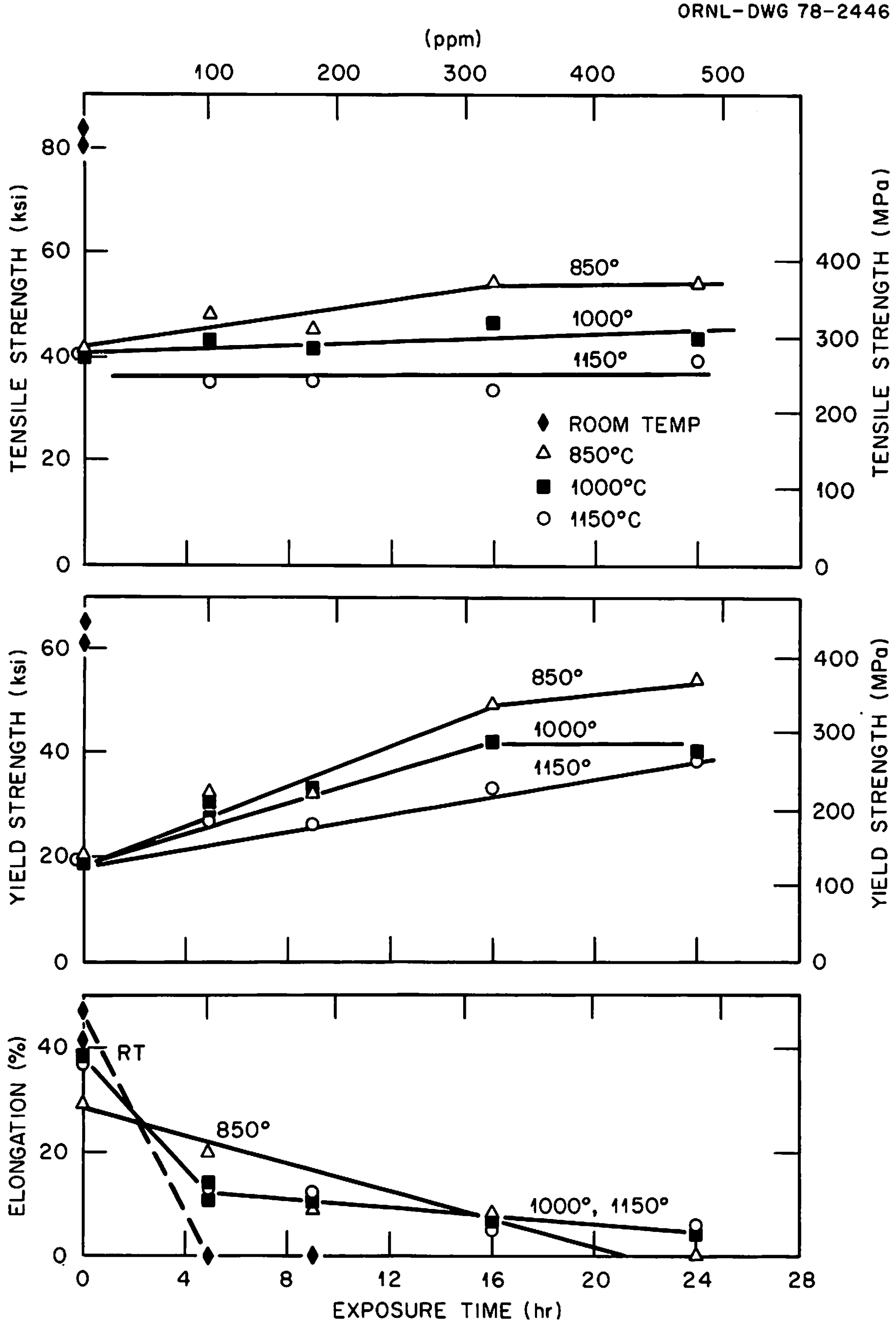

Fig. 4. Tensile Properties of TZM Sheet Specimens as Functions of Exposure Time at 1150°C and 1.3 mPa Oxygen.

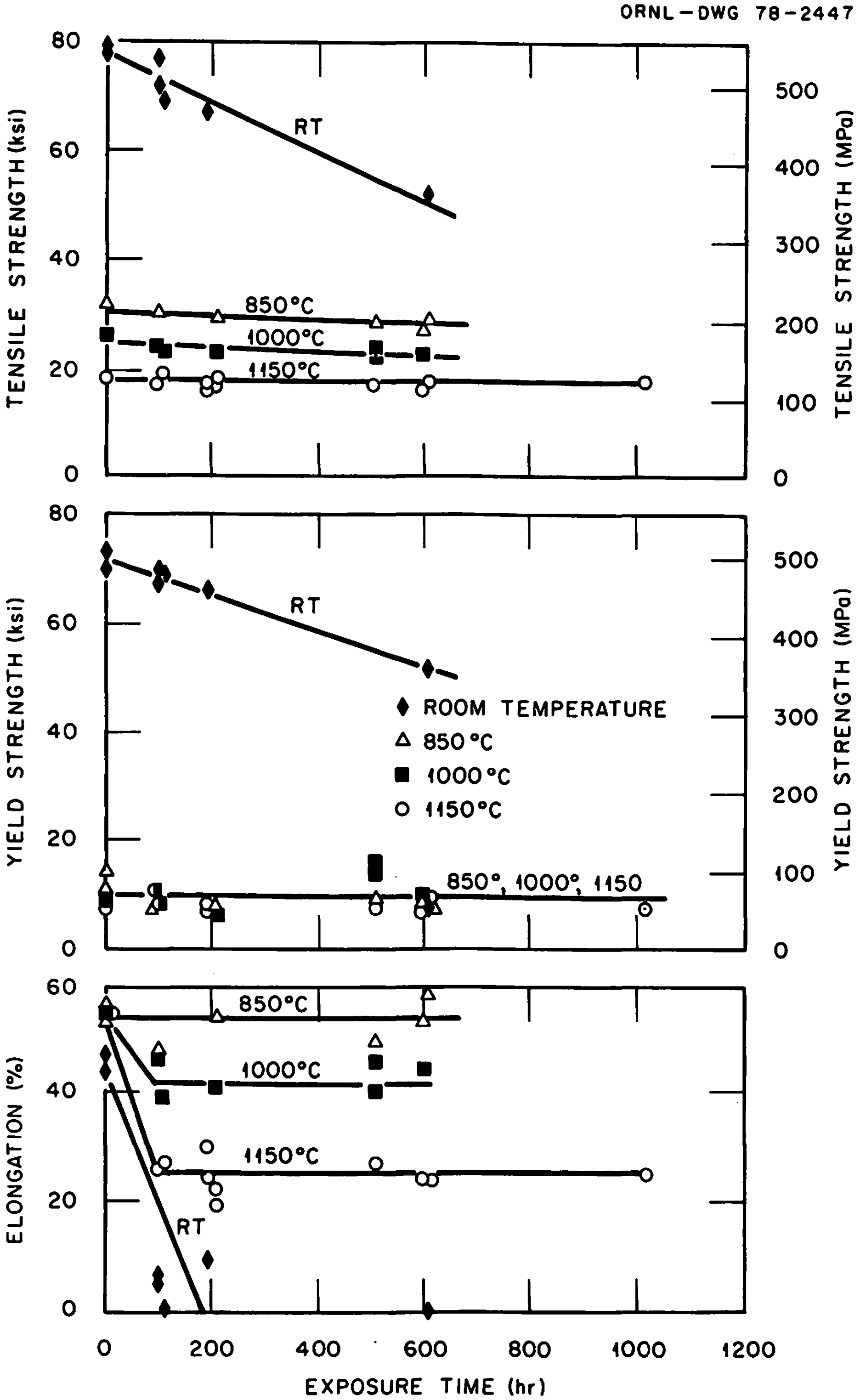

Fig. 5. Tensile Properties of Molybdenum Sheet Specimens as Functions of Exposure Time at 1150°C and 1.3 mPa Oxygen.

molybdenum loses its ductility after 200 h exposure. At elevated temperatures, the strength is virtually unaffected by exposure; however, the ductility shows an initial drop at 1000 and 1150°C but not at 850°C. Beyond 100 h exposure, the ductility at elevated temperatures is not further affected (Fig. 5).

Figure 6 shows the similar plot for the molybdenum control specimens aged at 1150°C in high vacuum. The primary effect of the vacuum aging is the lowering of the ductility and strength at room temperature. However, the drop in ductility in this case is not as severe as in the oxidizing environment, where molybdenum lost its ductility within 200 h exposure (Fig. 5). The tensile properties at elevated temperatures do not appear to be affected by vacuum aging.

The embrittlement due to oxygen exposure can be best demonstrated by comparing tensile elongation and reduction of area as functions of test temperature (Fig. 7) for molybdenum specimens exposed for about 100 h in oxygen and vacuum. An exposure time of 100 h was selected for this comparison since longer exposures to oxygen produced no further change in ductility (Fig. 5). As compared with vacuum aging, the oxygen exposure raises the ductile-to-brittle transformation temperature (DBTT) by about 200°C, and also sharply decreases ductility above 950°C. The ductility drops to a minimum value of 10% at 1350°C. Note that the ductility is only slightly affected in the intermediate temperature range, 400 to 900°C.

Fracture Behavior

Scanning electron microscope (SEM) examination of the fracture of unexposed TZM specimens tested at room temperature showed features characteristic of brittle fracture [Fig. 8(a)], even though the ductility at fracture was 45 to 48%. The frequency of cleavage fracture, as characterized by river patterns and steps, appears to increase with lowering ductility and increasing oxygen content in the oxidized TZM. The oxidized specimens exhibited very little grain-boundary separation below 400 ppm O_2. Further increase in oxygen content significantly promotes the intergranular fracture, and the dominant fracture mode for

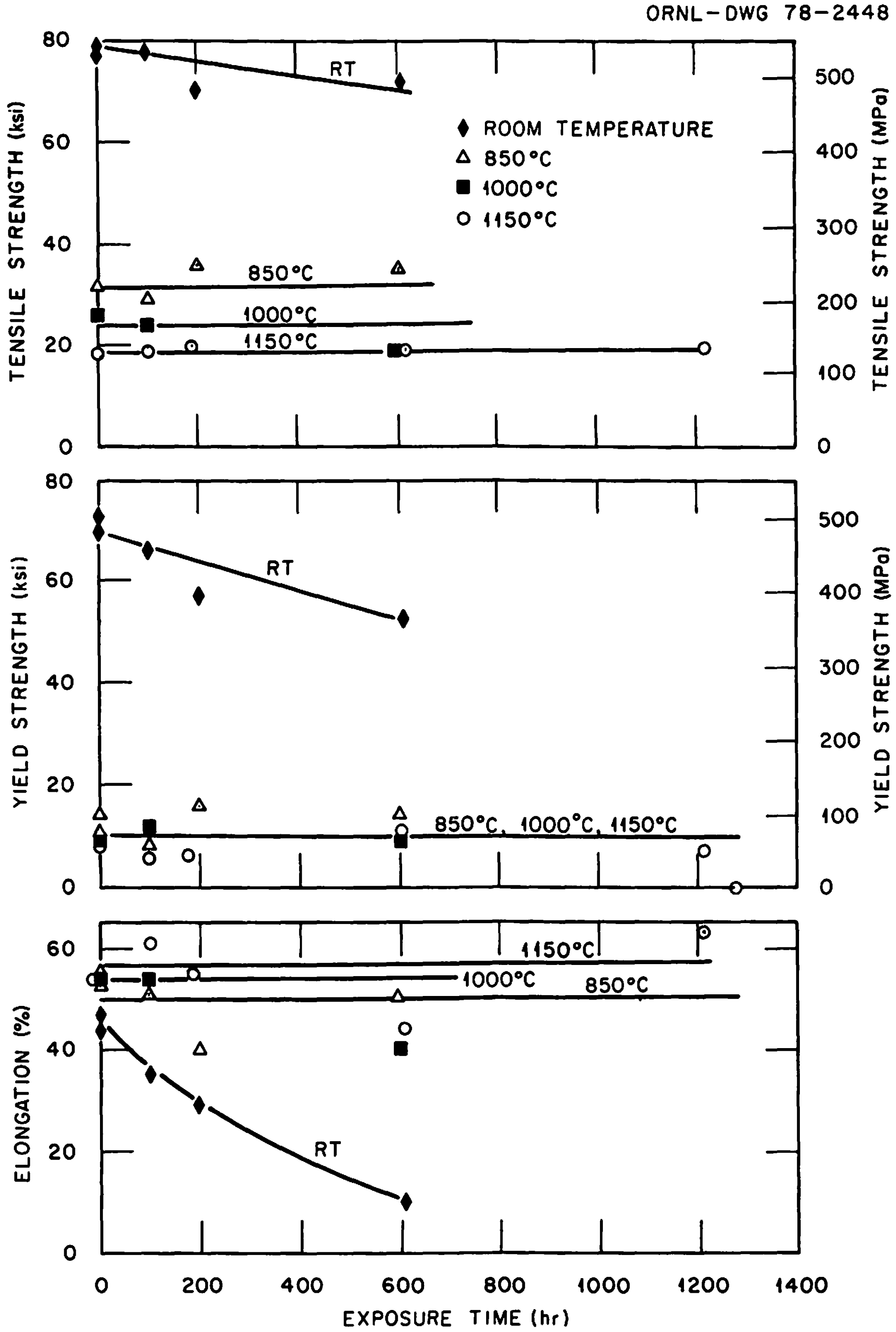

Fig. 6. Tensile Properties of Molybdenum Sheet Specimens as Functions of Aging Time at 1150°C in a Vacuum of 0.4 μPa.

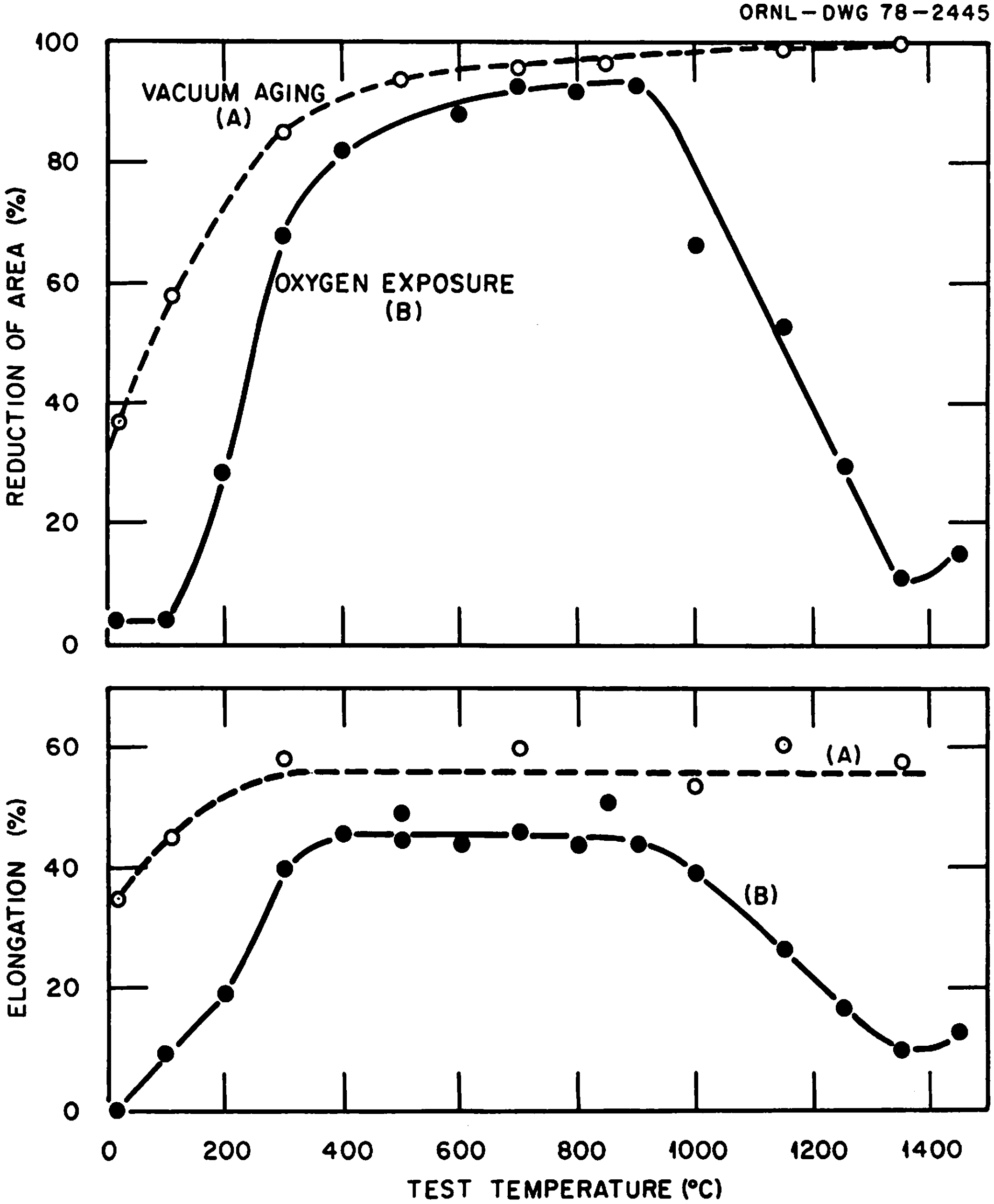

Fig. 7. Reduction of Area and Tensile Elongation as Functions of Test Temperature for Molybdenum Sheet Specimens Aged in Vacuum for 100 h at 1150°C and Exposed to 1.3 mPa Oxygen for 112 h at 1150°C.

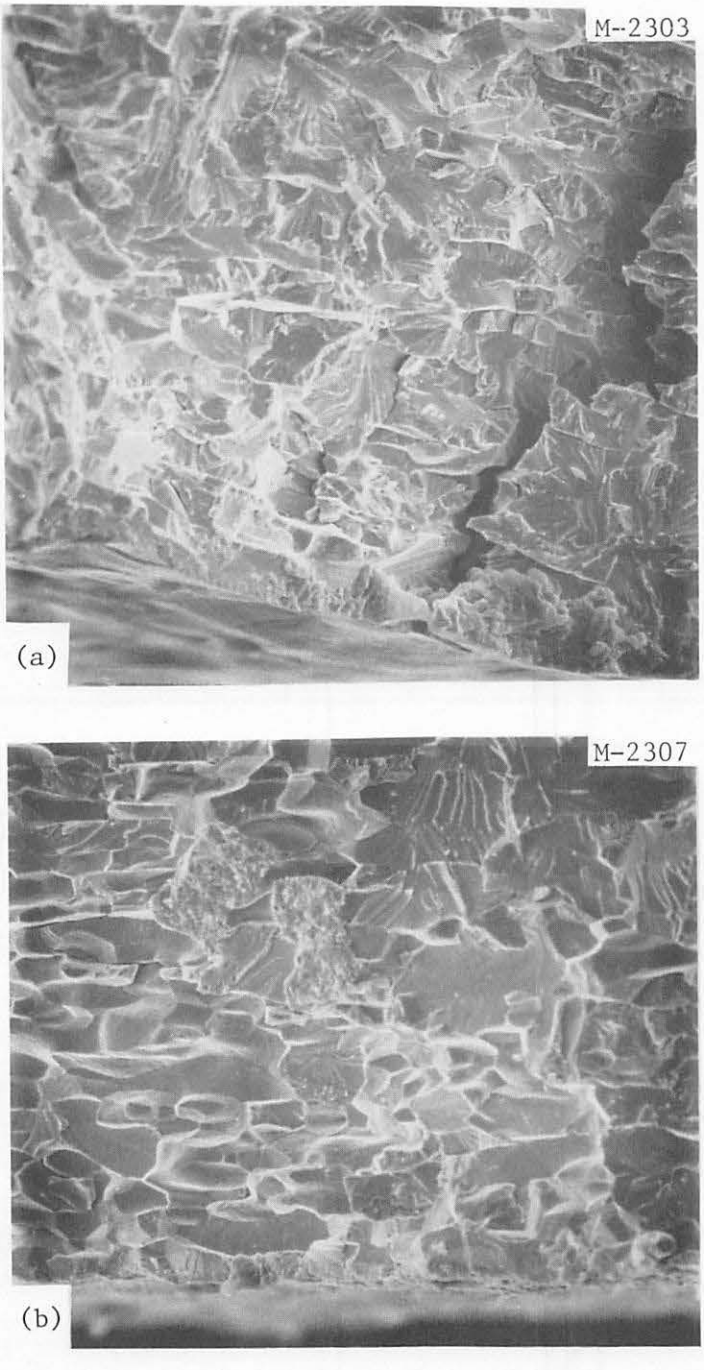

Fig. 8. Scanning Electron Microscope Fractographs of TZM Specimens Fractured at Room Temperature. 300×. (a) Unexposed specimen, 45% tensile elongation. (b) Exposed to oxygen for 100 h at 1150°C, fractured before macroscopic yielding.

the TZM specimen doped with 2100 ppm O was grain-boundary separation [Fig. 8(b)]. At 850°C and above, unexposed specimens exhibited ductile rupture with close to 100% reduction of area. The oxygen-exposed specimens fractured with two distinct regions: a ductile region in the center surrounded by a brittle fracture at the rim. The brittle rim was apparently failed by grain-boundary separation, as shown in Fig. 9.

As-recrystallized molybdenum specimens failed by a mixed mode of ductile fracture and brittle cleavage at room temperature. The ductile fracture was generally located in the central part of the fracture surface. Vacuum aging promotes brittle cleavage, with grain-boundary separation becoming more common at long aging times. On exposure to oxygen the room-temperature failure mode becomes predominantly intergranular, as shown in Fig. 10. At elevated temperatures, all the as-recrystallized and vacuum-aged specimens necked to a knife edge, as did the oxidized molybdenum tested at 850°C. Above 900°C, the fracture mode of oxidized specimens abruptly changed from ductile rupture to mixed intergranular separation (outer region) and ductile tearing (central region). Figure 11 shows the cross section of the fracture surface of such a specimen pulled at 1150°C. As the test temperature is further increased, the proportion of grain-boundary separation increases, and the latter mode dominates at 1350°C and 1450°C (Fig. 12). While room-temperature grain-boundary separation produced very smooth, specular surfaces (Fig. 10), the high-temperature tests produced some relatively smooth facets but also many rough and mottled facets (Figs. 11 and 12). Figure 12(b) shows a spot (indicated by arrows) where a chunk of material was torn out of one grain while remaining attached to another.

Metallographic examinations of molybdenum specimens near their fracture tips provided more information regarding the early stages of fracture. Figure 13(a) shows the fracture tip of a vacuum-aged specimen fracture with 44% elongation at 1150°C. A recrystallization process apparently occurred during deformation at 1150°C, so the boundaries were not well defined, and substructure was also visible within the grains. In contrast, cracks and voids were observed at the grain boundaries of the oxidized molybdenum specimens, particularly at high temperatures. At 850°C very few voids are generally located at the

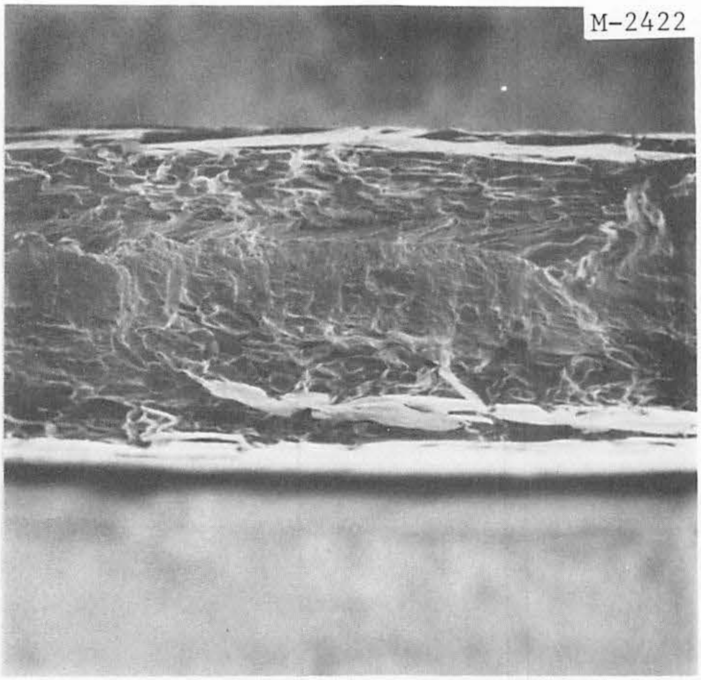

Fig. 9. Scanning Electron Microscope Fractograph of TZM Specimen Exposed to Oxygen for 9 h at 1150°C and Fractured at 1150°C; 12% Tensile Elongation. 100×.

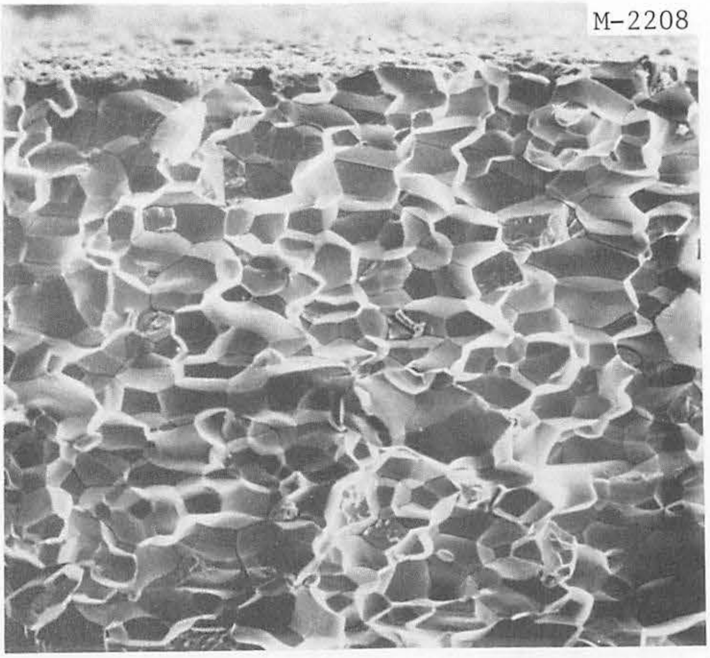

Fig. 10. Scanning Electron Microscope Fractograph of Molybdenum Specimen Exposed to Oxygen for 612 h at 1150°C and Fractured at Room Temperature. 300×.

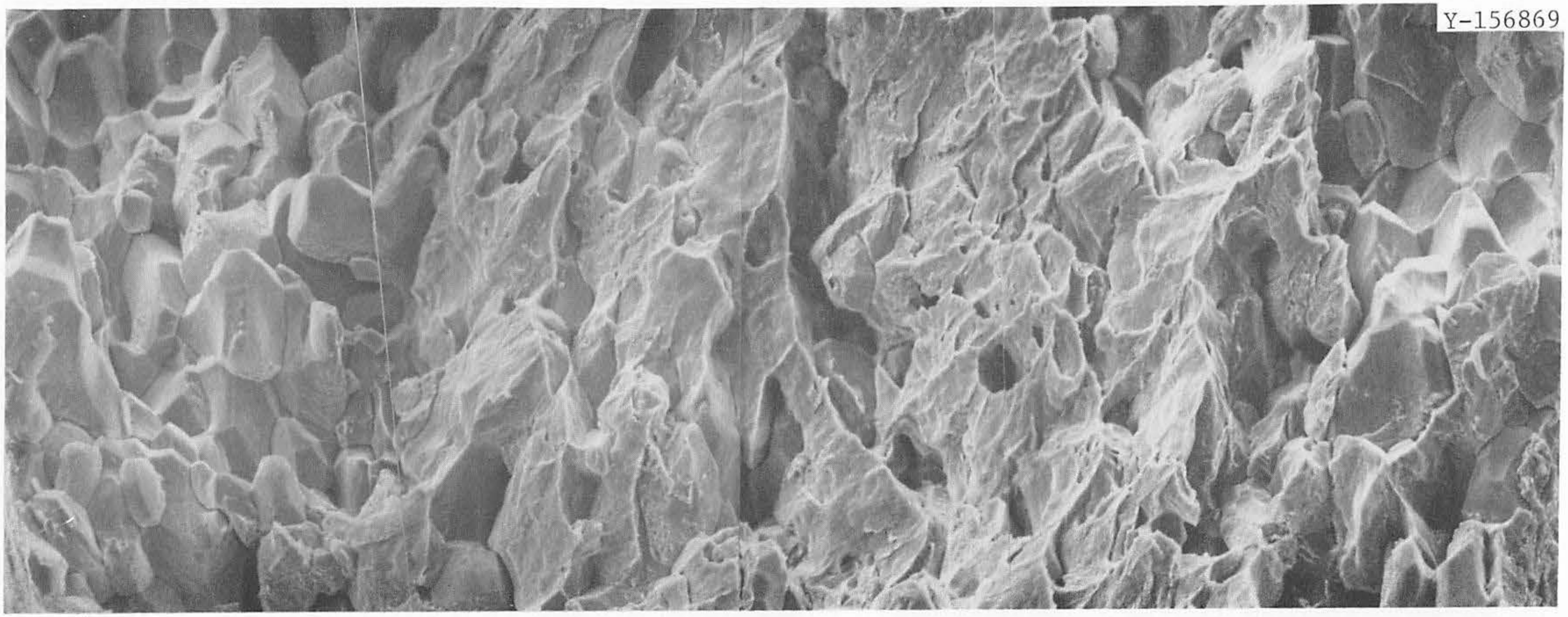

Fig. 11. Fracture Surface Across the Molybdenum Specimen Exposed to Oxygen for 600 h at 1150°C and Fractured at 1150°C; 24% Elongation. 500×.

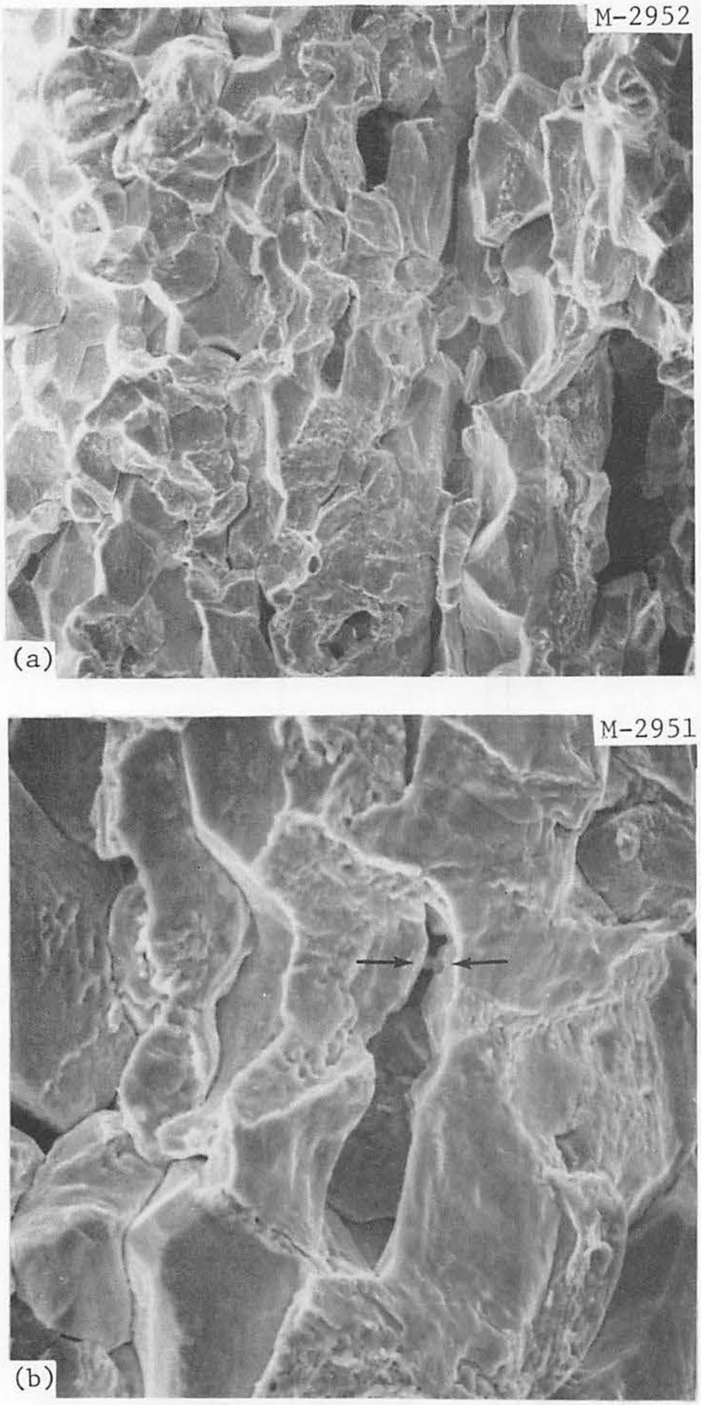

Fig. 12. Scanning Electron Microscope Fractographs of Molybdenum Specimen Exposed to Oxygen for 112 h at 1150°C and Fractured at 1350°C; 10% Elongation. (a) 300×. (b) 1000×. Arrows show material pulled by one grain from another during separation.

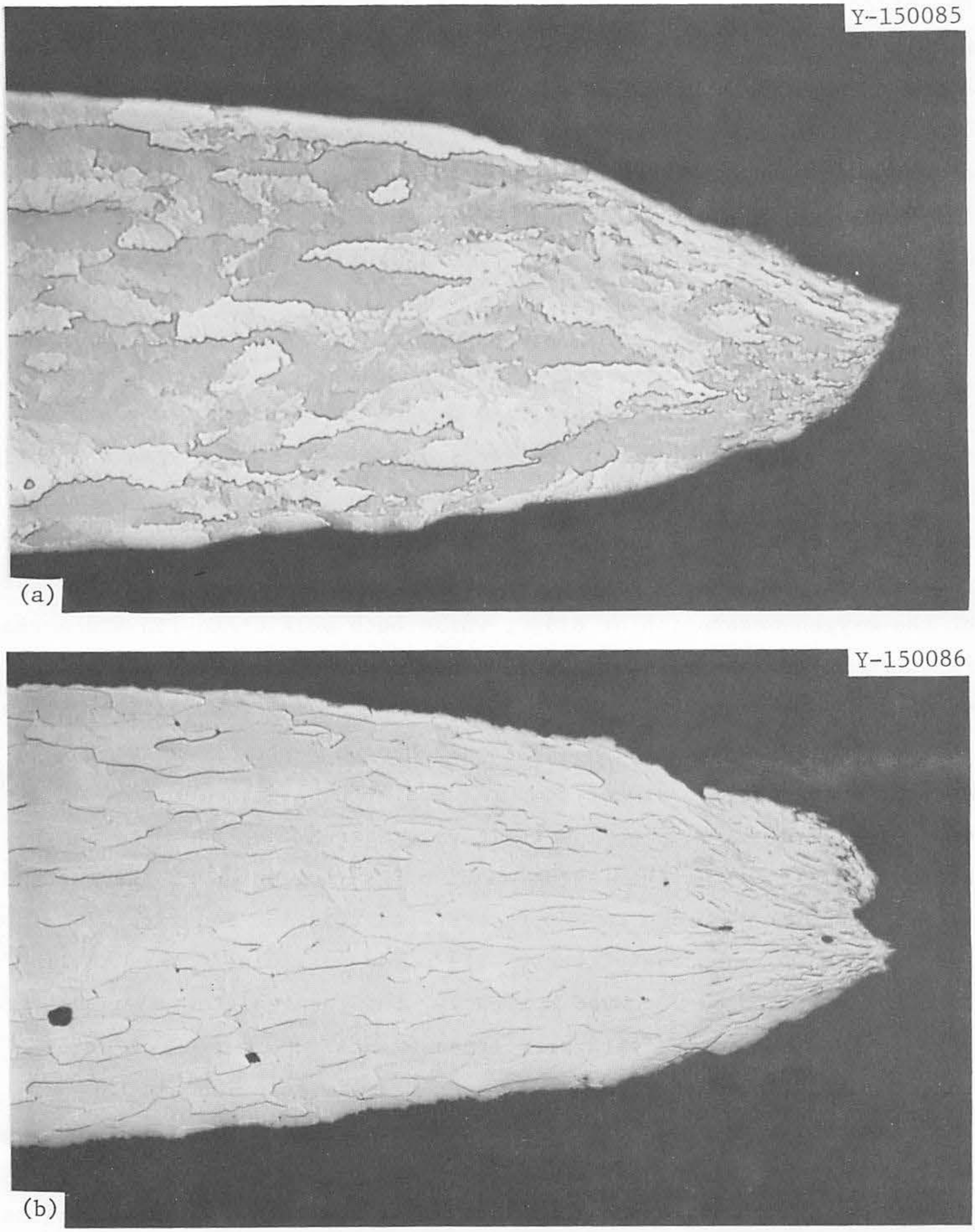

Fig. 13. Cross Section of Molybdenum Specimens Near Their Fracture Tips. 200×. (a) Vacuum aged for 806 h at 1150°C and fractured at 1150°C; 44% elongation. (b) Exposed to oxygen for 512 h at 1150°C and fractured at 850°C; 49% elongation.

triple points of the grain boundaries [Fig. 13(b)]. At 1000°C voids and microcracks have become prevalent but are small and closely associated with triple points. At 1150°C the metallographic cross section had a spongy appearance with relatively few small voids and predominantly cracks between grain boundaries [Fig. 14(a)]. At 1350 and 1450°C small cracks and voids are common but are not numerous until very close to the fracture [Fig. 14(b)]. There was no evidence of recrystallization during testing of the oxidized specimens at 1150 to 1450°C.

DISCUSSION

Exposure of TZM to low-pressure oxygen at elevated temperatures results in a steady pickup of oxygen. The kinetics of oxygen absorption has been found[3] to depend strongly on reaction temperature. Previous work[3] on internal oxidation of TZM in low-pressure oxygen, water vapor, and carbon monoxide showed that a diffusion process controls the kinetics of the oxygen absorption at 825°C, while both bulk diffusion and surface reaction affect the rate at 1000°C. Since the diffusivity and solubility of oxygen both increase exponentially with reaction temperature, it is reasonable that oxygen diffusion should become faster relative to the absorption process at higher temperatures. The linear increase of oxygen with time as shown in Fig. 1 certainly indicates that the rate-controlling step at 1150°C is the chemisorption of oxygen molecules at the surface.

The oxygen absorbed in TZM reacts with titanium and zirconium to form zones or oxide precipitates. The oxide particles formed at 1150°C were too small to be observed optically, but then existence was detected[3] previously from lattice parameter measurements. Formation of oxide removes titanium and zirconium atoms from solid solution and thus increases the oxygen solubility and concentration in solution, particularly near the specimen surface. Since the standard free energies of formation[4] of titanium and zirconium oxides are much more negative than

---

[3] C. T. Liu and H. Inouye, "Internal Oxidation and Mechanical Properties of TZM-Mo Alloy," *Metall. Trans.* 5: 2515–25 (1974).

[4] J. F. Elliot and M. Gleiser, *Thermochemistry for Steel Making*, Vol. 1, Addison-Wesley, Reading, Mass., 1960.

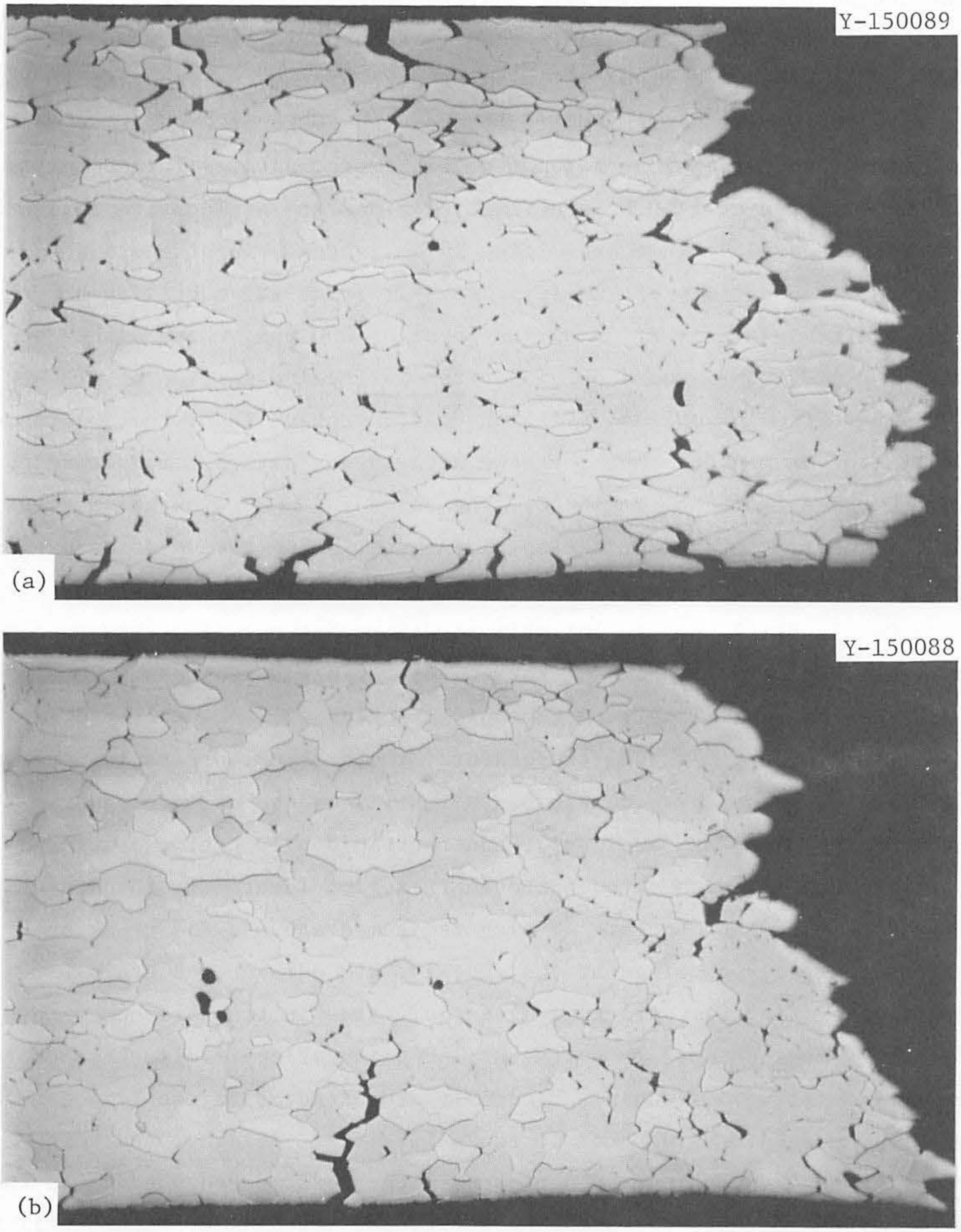

Fig. 14. Cross Section of Molybdenum Specimens Near Their Fracture Tips. 200×. (a) Exposed to oxygen for 512 h at 1150°C and fractured at 1150°C; 27% elongation. (b) Exposed to oxygen for 112 h at 1150°C and fractured at 1350°C; 10% elongation.

those of their carbides, it becomes thermodynamically feasible for the carbide particles to dissociate and free more titanium and zirconium to associate with oxygen. As a result, decarburization, as indicated in Fig. 1, could occur by diffusion of carbon from the interior to the surface and reaction with chemisorbed oxygen to form CO gas.

The fine dispersion of zones or oxide precipitates formed during oxygen exposure at 1150°C effectively impedes the dislocation motion and hardens the grain volume, resulting in an increase in strength and decrease in ductility of TZM (Fig. 4). It loses its ductility at elevated temperatures at an oxygen level of 500 ppm, which agrees well with the previous results obtained from internal oxidation of TZM at 850 and 1000°C in various oxidizing environments. Thus, the tolerance of TZM for oxygen does not increase with the oxidation temperature in the range from 825 to 1150°C. The hardening due to oxygen absorption is not uniform throughout the specimens and is indicative of an oxygen gradient near the surface. On tensile testing, the center of the specimen is still ductile and able to deform extensively, thus causing a stress concentration in the hard outer region. When this stress reaches a critical level, macroscopic cracking will be developed in the outer region. At room temperature, the critical stress is determined by the cleavage strength of the matrix or the grain boundary (depending on the oxygen level), and the rapid propagation of cracks from the outer region through the inner region lowers the total ductility of the oxidized specimens. At elevated temperatures, the cracking stress is solely governed by the cohesive strength of the grain boundaries (Fig. 9). Cracking again initiates in the hard outer case, but the cracks do not propagate until considerable yielding has occurred in the inner region. This was clearly demonstrated in the 1150°C tests of TZM exposed to oxygen for 16 to 24 h. After yielding, the hard case fractured, causing a sharp drop in the load, corresponding to the decrease in load-bearing area. However, failure did not occur until the center had necked down and suffered ductile rupture with concurrent elongation at the neck.

The embrittlement due to dispersion of fine oxides can be reduced through proper heat treatment at high temperatures.[3,5] To demonstrate this, a series of TZM specimens was first exposed to oxygen at 1.3 mPa for 100 h at 1150°C (∿2100 ppm O), then heat-treated at 1700°C for 15 min in vacuum. While untreated specimens fractured within the elastic range at all test temperatures, the heat-treated specimen exhibited 4% elongation at room temperature. The increase in ductility is attributed to the coarsening of oxide precipitates by aging.

Recent work of Srivastava and Siegle[6] has indicated that the oxygen solubility in molybdenum is extremely low, <1 ppm at 1150°C. This suggests that exposure to oxygen should not affect the bulk concentration of oxygen in molybdenum specimens. This is apparently consistent with our vacuum fusion analysis (Table 2), indicating no systematic change of oxygen content in molybdenum with exposure.

Nevertheless, the evidence obtained so far indicates that a trace amount of oxygen had gone into the molybdenum specimens through grain-boundary penetration during oxygen exposure at 1150°C. First, some particles that have the same appearance as the oxide film have been observed at grain boundaries near the surface of the exposed specimens (Fig. 2). Second, exposure to oxygen promotes grain-boudnary fracture in molybdenum (Fig. 10); as a result, the oxidized specimens show a higher DBTT and lower ductility above 900°C (Fig. 7). The change in tensile properties and fracture behavior is not simply due to the aging effects at 1150°C, because thermal aging in vacuum only moderately reduces ductility at room temperature and does not affect the ductility at high temperatures (Figs. 6 and 7). The DBTT of commercially pure molybdenum is slightly below room temperature, so any change in

---

[5] C. T. Liu, H. Inouye, and R. W. Carpenter, "Structural and Mechanical Properties of Internally Oxidized Ta–8 Pct W–2 Pct Hf (T-111) Alloy," *Metall. Trans.* 4: 1839–50 (1973).

[6] S. C. Srivastava and L. L. Seigle, "Solubility and Thermodynamic Properties of Oxygen in Solid Molybdenum," *Metall. Trans.* 5: 49–52 (1974).

metallurgical parameters[7–9] may significantly affect its ductility at room temperature. The low ductility of the control specimens is apparently due to the increase in grain size on vacuum aging at 1150°C, which raises the DBTT of molybdenum above room temperature. The increase of DBTT by grain growth has been observed in other bcc metals and alloys, such as steel.[10]

The low ductility and brittle fracture of oxygen-exposed molybdenum specimens can be explained in terms of migration and presence of oxygen at the grain boundaries. At low temperatures, the grain boundaries of molybdenum are quite brittle and form potential sites for crack initiation. The presence of oxygen at the boundaries increases their brittleness; as a result, the oxygen exposure promotes the intergranular fracture and raises the DBTT by 200°C (Fig. 7). This observation agrees with that of Olds and Rengstorff[11] who reported an increase in DBTT of molybdenum from —80 to 180°C with an addition of $\sim$10 ppm O. In the intermediate temperature range, 400 to 900°C, the grain boundaries of oxygen-exposed molybdenum apparently are ductile enough that they can deform extensively without nucleation of cracks. Thus, the oxygen exposure has little effect on the ductility of molybdenum from 400 to 900°C. The mobility of oxygen increases exponentially with temperature, and eventually the diffusion rate of oxygen is high enough to match the deformation rate of grain boundaries during strain at elevated temperatures. In this case, the molybdenum is progressively embrittled with increasing temperature, by concentration of more oxygen by diffusion to the grain boundaries and

---

[7] R. P. Carreker, Jr., and R. W. Guard, "Tensile Deformation of Molybdenum as a Function of Temperature and Strain Rate," *Trans. Metall. Soc. AIME* 206, 178–84 (1956).

[8] E. M. Passmore, "Correlation of Temperature and Grain Size Effects in the Ductile-Brittle Transition of Molybdenum," *Philos. Mag.* 8: 441–50 (1965).

[9] R. T. Ault and J. W. Spretnak, "Initial Yielding and Fracture in Notched Sheet Mo," *Int. J. Mech. Sci.* 7: 87–102 (1965).

[10] J. R. Low, Jr., *Relation of Properties to Microstructure*, American Society for Metals, Metals Park, Ohio, 1963, p. 63; *Fracture of Solids*, Interscience, New York, 1963, p. 197.

[11] L. E. Olds and G.W.P. Rengstorff, "Effects of Oxygen, Nitrogen, and Carbon on the Ductility of Cast Molybdenum," *Trans. Am. Inst. Min. Metall. Pet. Eng.* 206: 150–55 (1956).

crack tips, where the triaxial states of stress are generated during plastic deformation. This embrittlement, which is reflected by the ductility minimum at a certain temperature, is generally referred to as slow-strain-rate embrittlement[12] and has been observed in many bcc metals[13,14] such as steel, V, Nb, and Ta.

To verify this embrittlement mechanism in molybdenum, a pair of tensile specimens were heat-treated for 100 and 112 h separately in vacuum and 1.3 mPa oxygen and then impact-tested at 1350°C at a velocity of 85 m/s (280 fps). In terms of strain rate, this velocity gives an approximate rate of 5 km/min, which is higher than the tensile strain rate (2.5 mm/min) by more than six orders of magnitude. The vacuum-aged specimen had 50% elongation and the oxygen-exposed specimen had 56% elongation, and both specimens showed ductile rupture with close to 100% reduction of area. This comparison clearly demonstrates that oxygen exposure does not impair the ductility of molybdenum at 1350°C when deformed at the high strain rate. From this result we conclude that the ductility minimum in Fig. 7 for the oxygen-exposed molybdenum specimens is due to the dynamic embrittlement effect — that is, migration and concentration of oxygen to grain boundaries during slow-strain-rate testing — and that this embrittlement can be reduced or totally eliminated by an increase in strain rate.

Metallographic examination of the oxidized molybdenum tensile specimens reveals the formation of numerous cracks along grain boundaries at 1150 to 1450°C, whereas only a few voids associated with triple points are evident at 850°C (Figs. 13 and 14). To understand the nucleation and propagation of cracks in the oxygen-doped molybdenum, successive tensile tests were conducted on a single specimen at 1350 and 800°C. The specimen, which was exposed to 1.3 mPa O_2 for 112 h, was

---

[12] A. R. Troiano, "The Role of Hydrogen and Other Interstitials in the Mechanical Behavior of Metals," *Trans. Am. Soc. Met.* 52: 54–80 (1960).

[13] J. R. Donoso and R. E. Reed-Hill, "Slow Strain Rate Embrittlement of Niobium by Oxygen," *Metall. Trans.* 7A: 961–65 (1976).

[14] J. R. Donoso, A. T. Santhanam, and R. E. Reed-Hill, "Slow Strain-Rate Embrittlement in Metals," pp. 1174–78 in *Proc. 2nd Int. Conf. Mechanical Behavior of Materials, 16–20 August 1976,* American Society for Metals, Metals Park, Ohio, 1976.

first strained 8% at 1350°C, cooled to 800°C (within 3 min) while under a load greater than the yield stress, then pulled to fracture at 800°C. The ductility at 800°C was decreased moderately by the prestressing. Elongation decreased from 44% in an 800°C test without prestressing to 33% in the latter test, and reduction of area from 92 to 59%. The microstructure closely resembled that of an uninterrupted 1150°C test, except that larger voids were formed between grain-boundary facets (Fig. 15). The observation of numerous large voids after prestressing at 1350°C is consistent with the predictions from the dynamic embrittlement mechanism. According to this mechanism, cracks will be nucleated at triple points at 1350°C as a result of the migration and concentration of oxygen at the grain boundaries, the region of high triaxial stresses. The nucleated cracks would propagate and cause brittle failure along the grain boundaries if the oxidized specimen is pulled without interruption at 1350°C. However, the reduction of test temperature from 1350 to 800°C drastically reduces the supply and concentration of oxygen at grain boundaries and crack tips, so the nucleated cracks in this case cannot propagate in a brittle manner; instead, they grow into large voids through extensive plastic deformation. The final rupture of the duplex-tested specimen appears to be due to shearing and coalescence of voids (Fig. 15).

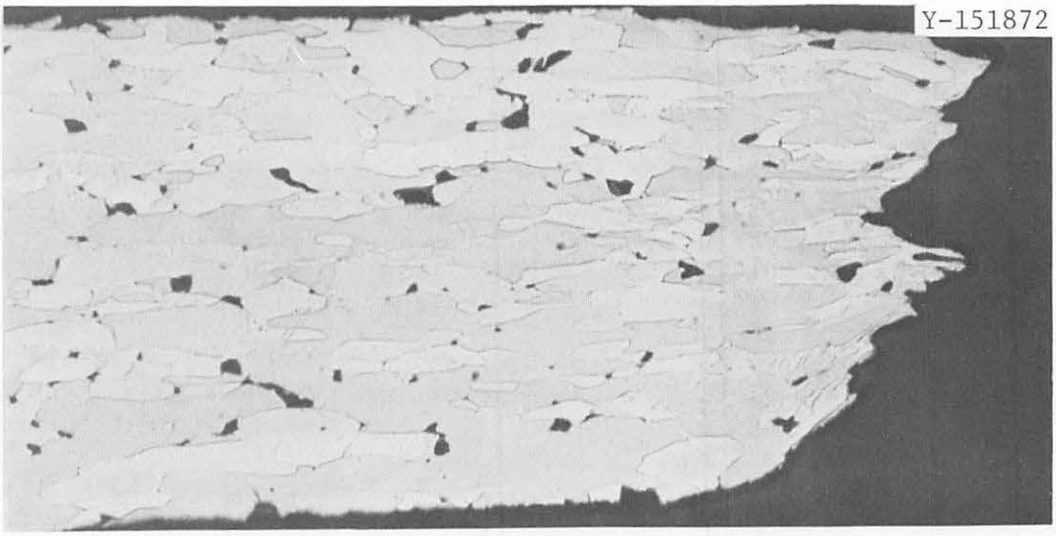

Fig. 15. Fracture Tip of Molybdenum Specimen Exposed to Oxygen for 112 h at 1150°C and Then Strained 8% at 1350°C and Fractured at 800°C (Duplex Test).

EVALUATION AND SUMMARY

Combining past and present results of environmetnal exposures and tensile tests of molybdenum and TZM, we are now in a position to evaluate the molybdenum-base alloys as structural members for closed-cycle energy systems whose environments usually contain low-pressure active gases. Exposure of TZM to oxidizing environments containing oxygen, water vapor, or carbon monoxide at 825 to 1150°C results in a pickup of oxygen and reduction in its tensile ductility. Exposed TZM loses its ductility at a level of 500 ppm O, independent of exposure temperature. The embrittlement is due to the formation of titanium and zirconium oxide zones or precipitates, which harden TZM and promote brittle fracture by cleavage and grain-boundary separations. The ductility of embrittled TZM increases with heat treatment at 1700°C. The increase in ductility is attributed to the coarsening of the oxide precipitate.

Kinetics of oxygen absorption in TZM depends largely on the reaction temperature. At 825°C or below, the oxygen absorption is controlled by a bulk diffusion process, so its rate depends strongly on the reaction temperature but not on the gas pressure and species. Our kinetic and tensile data predict that the ductility of TZM specimens with a thickness of 0.51 mm (0.020 in.) could fall below 5% at 825°C after exposure to oxidizing environments for 20,000 h (or 2.3 years). However, both bulk diffusion and chemisorption processes affect the oxygen absorption rate at 1000°C, and TZM is embrittled after 100 h exposure in 1.3 mPa (1×10^{-5} torr) oxygen or after 1500 h exposure to 1.3 mPa CO at 1000°C. At 1150°C, oxygen absorption is controlled primarily by chemisorption, and its rate is so fast that TZM loses its ductility in 5 to 24 h when exposed at 1150°C. From these results, we conclude that TZM is generally not suitable for use as a structural material for closed-cycle energy systems. If it must be used in certain cases, the operation temperature should be kept below 825°C.

Unalloyed molybdenum responds to the oxidizing environment quite differently from TZM. The molybdenum (containing no active elements such as titanium and zirconium) shows no internal oxidation in the oxidizing environment at 1150°C. Also, the oxygen solubility in molybdenum is so low that the bulk concentration of oxygen is not affected by exposure to low-pressure oxygen. However, our results indicate that a trace amount of oxygen penetrates into molybdenum through its grain boundaries. The grain-boundary penetration raises the DBTT of molybdenum by 200°C and lowers the ductility at temperatures above 900°C. The ductility minimum observed at 1350°C (Fig. 7) is due to dynamic embrittlement effects — namely, migration and concentration of oxygen by diffusion to grain boundaries and crack tips, where the high triaxial states of stress are generated during plastic deformation. Testing at a higher strain rate totally eliminates this embrittlement. The ductility of oxygen-exposed molybdenum is not affected in the temperature range from 400 to 900°C. In fact, the exposed molybdenum had more than 10% tensile elongation at temperatures above 100°C (Fig. 7), demonstrating that molybdenum itself is not severely embrittled in oxidizing environments.

From the results obtained from the study of environmental effects on molybdenum and TZM, we believe that molybdenum-base alloys can be used as structural materials for closed-cycle energy systems with contaminated environments, if they are alloyed properly. The prerequisites for a proper alloying element in molybdenum are: (1) The alloying element should not be an oxide former in molybdenum; that is, internal oxidation should not occur in the alloy exposed to oxidizing environments. (2) The element should be an effective strengthener of molybdenum. A brief survey[15-20]

---

[15] R. I. Jaffee, D. J. Maykuth, and R. W. Douglas, "Rhenium and the Refractory Platinum-Group Metals," pp. 383–465 in *Refractory Metals and Alloys*, Vol. II, ed. by M. Semchyshen and J. J. Harwood, Interscience, New York, 1961.

[16] G. A. Geach and J. E. Hughes, "The Alloys of Rhenium with Molybdenum or with Tungsten and Having Good High Temperature Properties," pp. 245–53 in *Plansee Proceedings 1955 — Sintered High-Temperature and Corrosion-Resistant Materials*, Metallwerk Plansee Ges. M.B.H., Reulte/Tyrol, Austria, 1956.

[17] W. D. Klopp and W. R. Witzke, "Mechanical Properties of Electron-Beam-Melted Molybdenum and Dilute Mo-Re Alloys," *Metall. Trans.* 4: 2006–10 (1973).

[18] J. R. Stephens and W. R. Witzke, *Alloy Hardening and Softening in Binary Mo Alloys as Related to Electron Concentration*, NASA-TN-D-6810 (May 1972).

[19] A. C. Schaffhauser, ORNL, "Ductility of Welded Molybdenum-Rhenium Alloys," unpublished results.

[20] O. Kubachewski, E.L.C. Evans, and C. B. Alcock, *Metallurgical Thermochemistry*, 4th ed. Pergamon Press, 1967.

of the physical and mechanical properties of molybdenum-rhenium alloys indicates that rhenium would satisfy these conditions. In addition, alloying molybdenum with rhenium improves its fabricability, weldability, and ductility at low temperatures. Therefore, we strongly recommend characterization of molybdenum-rhenium alloys in contaminated environments for closed-cycle energy systems, such as high-temperature gas-cooled reactors and radioisotopic power systems for space applications.

ACKNOWLEDGMENT

The authors gratefully acknowledge the encouragement of A. C. Schaffhauser as program coordinator. Special thanks are extended to T. J. Henson for scanning electron microscopy, W. H. Farmer for metallography, E. H. Lee for impact testing, J. H. DeVan, J. R. Keiser, and R. L. Klueh for manuscript review, and S. Petersen for technical editing, and L. J. Renfro of the Reports Office for publication assistance.

ORNL-5431
Distribution
Category UC-25

INTERNAL DISTRIBUTION

1–2. Central Research Library
3. Document Reference Section
4–5. Laboratory Records Department
6. Laboratory Records, ORNL RC
7. ORNL Patent Office
8. S. L. Bennett
9. J. Bentley
10. A. J. Caputo
11. R. W. Carpenter
12. J. V. Cathcart
13. O. B. Cavin
14. S. A. David
15. J. H. DeVan
16. M. L. Grossbeck
17. D. E. Harasyn
18. R. F. Hibbs
19–21. M. R. Hill
22. J. D. Holder
23. J. A. Horak
24–28. H. Inouye
29. J. R. Keiser
30. Eal H. Lee
31. J. S. Lin
32–41. C. T. Liu
42. R. E. Pawel
43. T. C. Reilly
44. A. F. Rowcliffe
45–47. A. C. Schaffhauser
48. G. M. Slaughter
49. V. J. Tennery
50. P. F. Tortorelli
51. C. L. White
52. F. W. Wiffen
53. Felix Yen
54. R. W. Balluffi (Consultant)
55. P. M. Brister (Consultant)
56. W. R. Hibbard, Jr. (Consultant)
57. M. J. Mayfield (Consultant)
58. N. E. Promisel (Consultant)
59. John Stringer (Consultant)

EXTERNAL DISTRIBUTION

60. AiResearch Manufacturing Company of Arizona, 402 South 36th Street, P.O. Box 5217, Phoenix, AZ 85010

J. E. McCormick

61. Battelle Memorial Institute, 505 King Avenue, Columbus, OH 43201

C. Alexander

62. Fairchild Space and Electronics Company, Germantown, MD 20767

A. Schock

63. General Electric Company, Materials Technology, Energy Systems Programs, 1 River Road, Schenectady, NY 12345

R. G. Frank

EXTERNAL DISTRIBUTION

64. General Electric Company, Nuclear Programs, P.O. Box 8661,
Philadelphia, PA 19101

E. W. Williams

65. Gulf Energy and Environmental Systems, P.O. Box 608, San Diego,
CA 92112

N. Elsner

66. Kirtland Air Force Base, NM 87117

Directorate of Nuclear Safety

67–68. Los Alamos Scientific Laboratory, P.O. Box 1663, Los Alamos,
NM 87545

S. E. Bronisz
S. Hecker
Lynn B. Lundberg

69. Minnesota Mining and Manufacturing Company, 2501 Hudson Road,
St. Paul, MN 55119

E. F. Hampl

70. Monsanto Research Corporation, P.O. Box 32, Miamisburg, OH 45342

E. W. Johnson

71. Sunstrand Energy Systems, 4747 Harrison Avenue, Rockford, IL 61101

E. Kreuger

72–73. Teledyne Energy Systems, 110 W. Timonium Road, Timonium, MD 21093

W. J. Barnett
W. Osmeyer

74–84. USDOE Division of Advanced Systems and Materials Production,
Washington, DC 20545

T. J. Dobry
T. J. Holleman
W. D. Kenney
A. P. Litman

J. J. Lombardo
B. J. Rock
C. O. Tarr
N. R. Thielke

EXTERNAL DISTRIBUTION

85–86. USDOE Office of Energy Research, Washington, DC 20545

R. N. Kostoff
L. C. Ianniello

87. USDOE Oak Ridge Operations Office, P.O. Box E, Oak Ridge, TN 37830

Research and Technical Support Division

88–315. USDOE Technical Information Center, P.O. Box 62, Oak Ridge, TN 37830
For distribution as shown in TID-4500 Distribution
Category UC-25 Materials